Molecular Therapy
Methods & Clinical Development
Original Article

Efficient in Utero Gene Transfer to the Mammalian Inner Ears by the Synthetic Adeno-Associated Viral Vector Anc80L65

Chin-Ju Hu, Master,[1,15] Ying-Chang Lu, Ph.D.,[1,2,15] Yi-Hsiu Tsai, Master,[2,3,15] Haw-Yuan Cheng,[3] Hiroki Takeda,[4] Chun-Ying Huang,[2] Ru Xiao,[5,6] Chuan-Jen Hsu,[11] Jin-Wu Tsai,[3,12] Luk H. Vandenberghe,[5,6,7,8,9] Chen-Chi Wu,[1,10] and Yen-Fu Cheng[2,3,13,14]

[1]Department of Otolaryngology, National Taiwan University Hospital, Taipei, Taiwan; [2]Department of Medical Research, Taipei Veterans General Hospital, Taipei, Taiwan; [3]Institute of Brain Science, National Yang-Ming University, Taipei, Taiwan; [4]Department of Otolaryngology-Head and Neck Surgery, Kumamoto University Graduate School of Medicine, Kumamoto City, Japan; [5]Grousbeck Gene Therapy Center, Schepens Eye Research Institute and Massachusetts Eye and Ear, Boston, MA, USA; [6]Ocular Genomics Institute, Department of Ophthalmology, Harvard Medical School, Boston, MA, USA; [7]Harvard Stem Cell Institute, Cambridge, MA, USA; [8]Broad Institute of MIT and Harvard, Cambridge, MA, USA; [9]Department of Ophthalmology, Harvard Medical School, Boston, MA, USA; [10]Department of Medical Research, National Taiwan University Hospital Biomedical Park Hospital, Hsinchu, Taiwan; [11]Department of Otolaryngology, Taichung Tzu Chi Hospital, Buddhist Tzu Chi Medical Foundation, Taichung, Taiwan; [12]Brain Research Center, National Yang-Ming University, Taipei, Taiwan; [13]School of Medicine, National Yang-Ming University, Taipei, Taiwan; [14]Department of Otolaryngology-Head and Neck Surgery, Taipei Veterans General Hospital, Taipei, Taiwan

Sensorineural hearing loss is one of the most common sensory disorders worldwide. Recent advances in vector design have paved the way for investigations into the use of adeno-associated vectors (AAVs) for hearing disorder gene therapy. Numerous AAV serotypes have been discovered to be applicable to inner ears, constituting a key advance for gene therapy for sensorineural hearing loss, where transduction efficiency of AAV in inner ear cells is critical for success. One such viral vector, AAV2/Anc80L65, has been shown to yield high expression in the inner ears of mice treated as neonates or adults. Here, to evaluate the feasibility of prenatal gene therapy for deafness, we assessed the transduction efficiency of AAV2/Anc80L65-eGFP (enhanced green fluorescent protein) after microinjection into otocysts *in utero*. This embryonic delivery method achieved high transduction efficiency in both inner and outer hair cells of the cochlea. Additionally, the transduction efficiency was high in the hair cells of the vestibules and semicircular canals and in spiral ganglion neurons. Our results support the potential of Anc80L65 as a gene therapy vehicle for prenatal inner ear disorders.

INTRODUCTION

Sensorineural hearing loss (SNHL) is one of the most common sensory disorders worldwide. According to the World Health Organization, over 5% of the population (466 million people) suffers from hearing loss. Additionally, approximately 2% of school-age children have mild or late-onset SNHL in one or even both ears.[1,2] Although SNHL is a high-prevalence disability, treatments are limited. Cochlear implantation is currently the main treatment option for severe to profound SNHL, but the outcomes vary significantly among recipients.

Gene therapy has become an attractive option in the exploration of potential biological treatments for SNHL. Various systems exist for the delivery of genetic constructs in gene therapy; these can be categorized into viral delivery systems and nonviral delivery systems. The advantages of viral delivery systems include their safety and higher transduction efficiency.[3–5] Additionally, many viral delivery systems are in clinical trials (clinicaltrials.gov: https://clinicaltrials.gov/ct2/home). Different serotypes of AAV exhibit different transduction efficiencies in specific target cells and tissues.[6] Several serotypes have previously been tested in inner ears, including AAV1, AAV2, AAV5, AAV6, AAV8, AAV9, AAV2.7m8, AAV8BP2, AAVrh.39, AAVrh.43, AAV-ie, and Anc80L65.[3,7–20,40,41,42]

Anc80L65 is predicted to be an ancestor of several AAV serotypes, including AAV1, AAV2, AAV8, and AAV9. Anc80L65 was initially reconstructed *in silico* from 75 capsid protein sequences of human and primate evolutionary lineages.[21] The innovative serotype Anc80L65 has demonstrated excellent performance in various cochlear cell types, including inner hair cells (IHCs), outer hair cells (OHCs), and supporting cells, when AAV is delivered in the neonatal

Received 18 March 2020; accepted 19 June 2020;
https://doi.org/10.1016/j.omtm.2020.06.019.

[15]These authors contributed equally to this work.

Correspondence: Chin-Ju Hu, Department of Otolaryngology, National Taiwan University Hospital, Taipei, Taiwan.
E-mail: ginniehu@g.harvard.com
Correspondence: Ying-Chang Lu, Department of Otolaryngology, National Taiwan University Hospital, Taipei, Taiwan.
E-mail: lu16889@gmail.com
Correspondence: Yi-Hsiu Tsai, Department of Medical Research, Taipei Veterans General Hospital, Taipei, Taiwan.
E-mail: iammolly730@gm.ym.edu.tw
Correspondence: Yen-Fu Cheng, Department of Medical Research, Taipei Veterans General Hospital, Taipei, Taiwan.
E-mail: yfcheng2@vghtpe.gov.tw

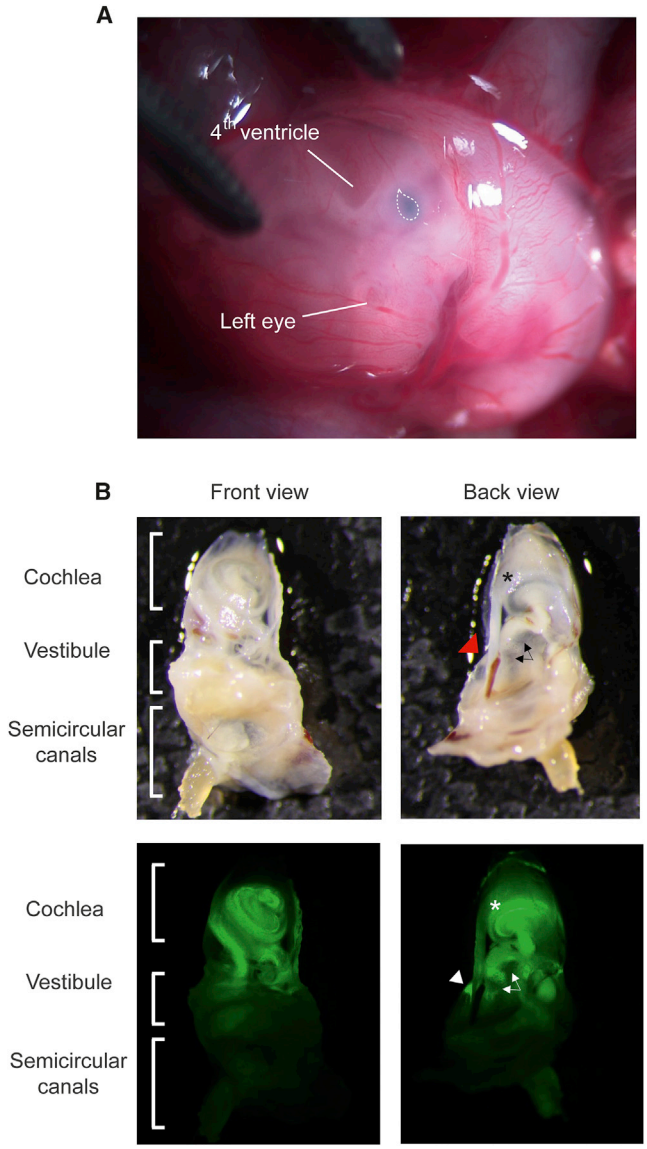

Figure 1. Schematic Diagram of the Method for Intrauterine Delivery into Embryonic Otocysts

(A) View of an E12 embryo after microinjection through the uterine wall. The tear-drop-shaped otocyst injected with a combination of Anc80L65 and dye is indicated by the dotted line. (B) Gross view of the distribution of the delivered eGFP in the inner ear at P28. The asterisk indicates the cochlea, the triangle indicates the transduced semicircular canals, and the arrows indicate the vestibule (saccule and utricle).

and/or adult stage.[3,13,15–18,22] Anc80L65 has also shown promise for the treatment of genetic deafness, including that induced by *Usch1c* or *Tmc1* mutations, in the postnatal stage in several mammalian models.[13,22] Considering the nature of the pathologic changes in some types of genetic deafness that can develop during the embryonic stage, we sought to investigate the efficacy of the synthetic AAV Anc80L65 for use at the embryonic stage.

RESULTS

Synthetic AAV2/Anc80L65 Efficiently Transduces the Embryonic Cochlear Sensory Epithelium

To evaluate the transduction efficiency of Anc80L65 in the embryonic cochlear sensory epithelium, we injected one microliter of synthetic AAV (2.52×10^{12} GC/mL) into one otocyst of each murine embryo at embryonic day 12 (E12; Figure 1). The survival rate of embryos in both the sham and Anc80L65 groups was 73.3%. The HC transduction efficiency was evaluated by the proportion of sensory HCs (marked by myosin VIIA) with enhanced green fluorescent protein (eGFP; carried by AAV) expression at the neonatal stage P7; HCs of sham-injected mice were used as a positive control for myosin VIIA and a negative control for eGFP signals (Figure 2A). Quantification analysis demonstrated that the average Anc80L65 transduction efficiency was approximately 90% in both IHCs and OHCs (Figures 2A and 2B; the IHC:OHC ratios were 79.3% ± 25.3%:86.5% ± 10.8% in the apex, 94.7% ± 7.6%:89.8% ± 8.3% in the middle, and 94.5% ± 8.1%:95.3% ± 2.8% in the base; n = 5 per turn). Besides, we also observed the transduction of supporting cells, including Deiters' cells, which are located below the OHCs, and Hensen's cells, which lie outside Deiters' cells (Figure 2C). A previous study noted that AAVs might access the contralateral ear via the cochlear aqueducts.[3] Interestingly, we did observe transduction of Anc80L65 in the contralateral ears of some mice, albeit to a much lower degree than that in the injected inner ears (Figure S1).

In Utero Delivery of Synthetic AAV2/Anc80L65 into the Embryonic Inner Ear Does Not Damage the Sensory Epithelium or Hearing Ability

To assess the safety of the synthetic AAV in the inner ear, we evaluated the loss of cochlear sensory epithelial cells, including IHCs and OHCs, at P7. Very little HC loss was found in mice in the AAV2/Anc80L65-CMV-eGFP-injected group and the sham surgery group injected with PBS (0.02% each). Similarly, no HC loss was observed in the vestibular areas.

To evaluate the possible adverse effects of *in utero* delivery of synthetic Anc80L65 on hearing, we assessed auditory brainstem response (ABR) thresholds (Figure 3A). Compared with mice in the PBS-injected sham surgery group (n = 5) and mice in the wild-type group not subjected to any surgical procedure (n = 6), mice in the group subjected to *in utero* delivery of AAV2/Anc80L65-CMV-eGFP (n = 5) exhibited no significant differences in the hearing threshold at any tested frequency (p values of 0.698, 0.842, 0.995, and 0.981 for the clicks and 8 kHz, 16 kHz, and 32 kHz tests, respectively; Figure 3B). These results indicate that synthetic Anc80L65 is safe with minimal effects on the embryonic cochlea.

Transduction Efficiency of AAV2/Anc80L65 in the Embryonic Vestibular Sensory Epithelium

The transduction efficiency in sensory HCs in the vestibular system was similarly evaluated by the ratio of eGFP-positive to myosin VIIA-positive cells at the neonatal stage (P7) after injection of the synthetic AAV into the otocysts of murine embryos. eGFP was expressed robustly in the vestibules and semicircular canals (Figures 4A and 4B). Robust

expression of eGFP in HCs indicated that Anc80L65 had high transduction efficiency in these cells. The transduction rates reached approximately 70% (71.4% ± 9.3%; n = 5) in semicircular canals and 90% (89.6% ± 7.8%; n = 5) in vestibules (Figure 4C).

Anc80L65 Transduces SGNs with High Efficiency

Moreover, we found that Anc80L65 transduces spiral ganglion neurons (SGNs) with high efficiency. To quantify the targeted SGNs, we assessed beta III tubulin expression. As shown in Figures 4D and 4E, both beta III tubulin and eGFP were expressed in SGNs, and the expression extended to the cochlear nerve. Neural fibers were also transduced by Anc80L65; fiber-like patterns of green fluorescence were observed around the nerve paths. The high transduction efficiency in SGNs (96.7% ± 1.7%; n = 3) demonstrates the potential of Anc80L65 for therapeutic use in neurological diseases.

DISCUSSION

In this study, we delivered a synthetic Anc80L65 AAV into the otocysts of murine embryos to investigate the feasibility of intrauterine gene therapy for inner ear disorders. Our results showed that synthetic Anc80L65 efficiently transduced the embryonic cochlear and vestibular sensory epithelium while causing minimal damage to sensory cells and minimal associated effects on hearing outcomes.

The method of *in utero* microinjection was established several years ago and has been confirmed to be safe for fetuses.[23] Furthermore, success in both murine models and human fetuses prompted Charles Coutelle to consider carefully revisiting prenatal gene therapy.[24] There are a few lines of reasoning supporting gene therapy at the embryonic stages. First, mutations in some genes may cause permanent damage even before birth. For example, deletion or mutation of *GJB2* and *SLC26A4* causes profound hearing loss at birth.[25,26] Therefore, treatment at the embryonic stages is beneficial for these kinds of mutations. Second, the early gestational fetus has a naive immune system, which makes viral vector- or transgene-encoded proteins more readily accepted by target cells in early embryos than by those in more mature tissues. This characteristic could substantially increase the efficiency of gene therapy.[27] Third, the blood-brain barrier is not mature during the embryonic stage; thus, molecular medicines can easily access brain tissues, which is advantageous for the treatment of neurological diseases, such as early-onset neuronopathic Gaucher disease.[28] However, as the majority of patients of genetic deafness involve recessive inheritance from parents who are heterozygous carriers for the disease-causing genetic variants, the identification and diagnosis of hearing loss are usually after birth. While this may represent a major barrier to implementing *in utero* treatment of hearing loss, *in utero* gene therapy may still be feasible and logical for those whose parents are both deaf and carrying bi-allelic recessive mutations of the same gene, as well as those with a deaf parent segregating a dominant mutation, when considering the clinical application in the future.

Several recent advances in intrauterine gene delivery into the inner ear have been reported. For example, Gubbels et al.[29] demonstrated that transfer of *Atoh1* into otocysts by electroporation could induce production of functional supernumerary HCs in the murine cochlea. In addition, *in utero* delivery of wild-type connexin 30 by electroporation into Cx30-knockout mice could ameliorate hearing loss.[30] Bedrosian et al.[20] first demonstrated the successful transduction of AAV1 in the otocysts. The application of AAV1 carrying the *MsrB3* gene to methionine sulfoxide reductase B-deficient ($MsrB3^{-/-}$) mice at the developmental stage was shown to restore both HC morphology and hearing function after birth.[31]

The synthetic Anc80L65 vector has been reported to be highly efficient in transducing target cells, especially different types of cells in the inner ear.[3,13,17,18,22] However, the transduction efficiency of this vector in the sensory epithelia of developing inner ear organs has not been reported. Similar to the findings reported by other researchers in neonatal or adult murine models,[3,7,11,14,15,18,32] our results revealed that Anc80L65 has an excellent ability to transduce both types of cochlear HCs (Figure 2B; Table 1). During development, cochlear HCs are derived from a subclass of prosensory domain cells that start to exit the cell cycle and form bipotent HC progenitors at E12.5.[33,34] We found that some supporting cells were eGFP-positive, indicating the ability of the vector to transduce the bipotent progenitors that eventually differentiate into either HCs or supporting cells.

In addition to cochlear HCs, vestibular HCs were also targeted by Anc80L65 with a high transduction efficiency. Vestibular disabilities occur in 10%–20% of infants with hereditary deafness, such as that associated with *COCH(DFNA9)*, *PJVK (DFNB59)*, *USH1C (DFNB18)*, *USH3*, and mtDNA 1555A > G (12S rRNA).[35–37] In addition to the treatment of hearing disorders, our findings suggest that Anc80L65 might be an ideal tool for the treatment of balance disorders resulting from hereditary hearing loss.

In this study, we demonstrated the transduction efficiency of Anc80L65 in the developing murine inner ears. However, some limitations must be considered before this method can be translated for application in humans. First, intrauterine microinjection of murine otocysts requires meticulous techniques, and adapting the developed microinjection technique for use in human embryos may be difficult. Second, hearing onset occurs at approximately 20 weeks of gestation in humans, while hearing onset occurs later in the postnatal stage in mice. Therefore, whether mouse disease models recapitulate the development of specific hearing and/or balance disorders in the human inner ear with regard to gene therapy requires careful study.

In summary, this study evaluated the ability of the synthetic AAV Anc80L65 to transduce embryonic otocysts. The high transduction efficiency in both cochlear and vestibular HCs, as well as SGNs indicates that the AAV Anc80L65 is a powerful gene delivery vector for the treatment of hereditary inner ear diseases *in utero*. The combination of prenatal treatment and effective AAV vector administration may enable the progression of gene therapy to the next level.

MATERIALS AND METHODS

AAV Production

The AAV2/Anc80L65-CMV-eGFP (2.52×10^{12} GC/mL) used in this study was packaged and purchased from the Gene Transfer Vector

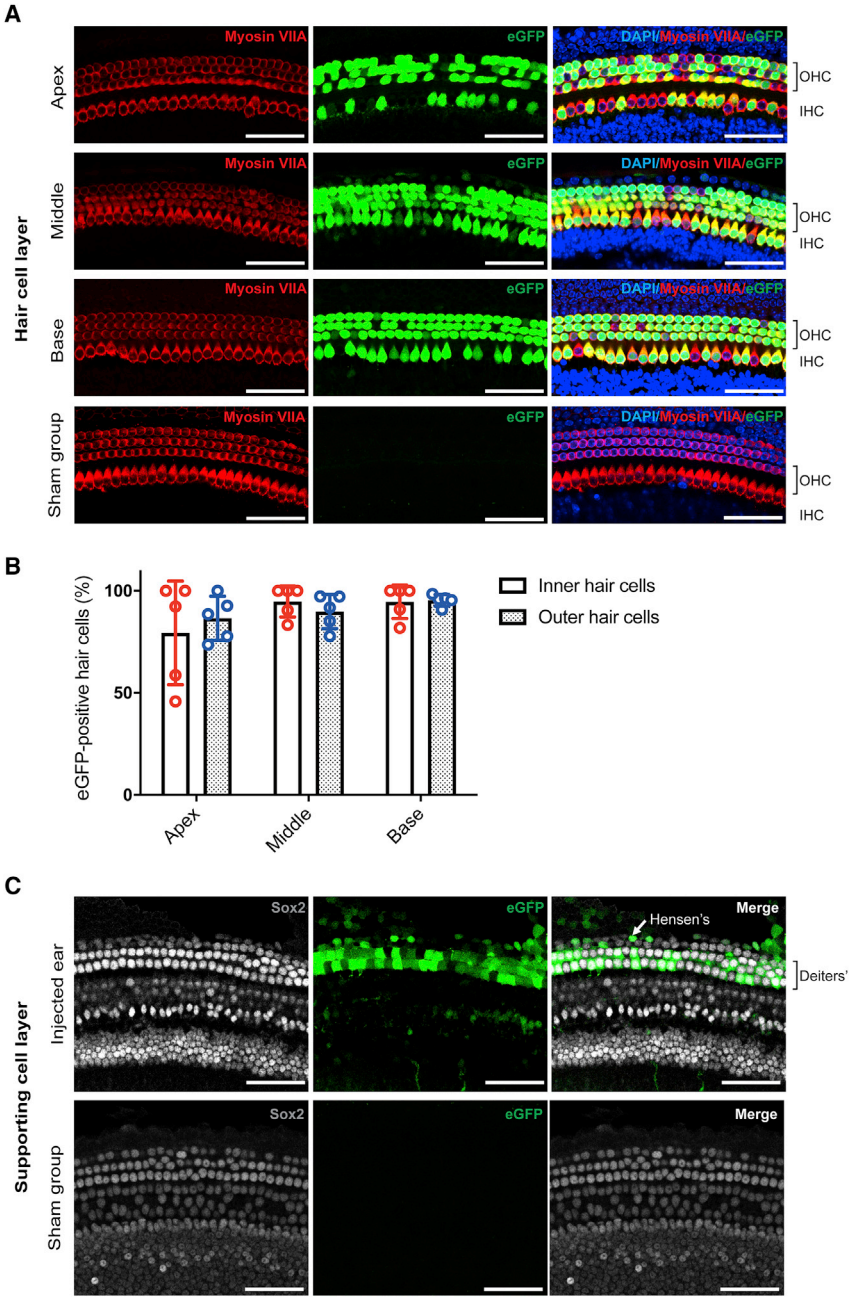

Figure 2. High Transduction Efficiency of Anc80L65 in Cochlear HCs

(A) The organ of Corti was mounted and divided into three parts: the apex, middle, and base. One row of IHCs and three rows of OHCs are clearly visible in the images. We compared myosin VIIA and eGFP expression between the Anc80L65-injected ears and the sham ears (injection of PBS solution only). Red indicates myosin VIIA, green indicates eGFP, and blue indicates DAPI. The scale bar represents 50 μm (n = 5). (B) The transduction efficiency was quantified in cochlear HCs with eGFP expression. No significant difference between the IHC and OHC transduction efficiency was found in any turn. (C) Supporting cell layer in a whole-mount preparation of the middle cochlear turn (same as in A). Sham ears were utilized as a positive control for Sox2 and a negative control for eGFP. Gray indicates Sox2-positive supporting cells, and green indicates eGFP. The scale bar represents 50 μm.

Core at the Grousbeck Gene Therapy Center, Massachusetts Eye and Ear (Boston, MA). The preparation procedures for this virus have been described previously.[21]

Animals

Pregnant wild-type C57BL/6 mice were purchased from BioLasco (Taiwan), and the main subjects in this study were the embryos in these mice. AAV2/Anc80L65-CMV-eGFP was delivered into embryonic otocysts until developmental day 12. All animal procedures were performed in accordance with protocols approved by the Institutional Animal Care and Use Committee (IACUC) of the National Taiwan University College of Medicine (approval number 20160337).

Surgical Procedure

All animal surgeries were conducted in a sterile environment in the laboratory of the Animal Center at National Yang-Ming University. The detailed surgical procedures used in this study were adopted from procedures described previously.[38] Briefly, pregnant C57BL/6 mice were anesthetized with gaseous 0.4% isoflurane (Panion & BF Biotech, Taipei, Taiwan) in a sealed cage for 3–5 min until they were deeply anesthetized. The mice were then removed from the cage and fitted with masks for continuous administration of gaseous isoflurane before the abdominal skin was incised along the midline for 1.5 cm. One otocyst in each embryo was microinjected by glass micropipette. Each otocyst in the experimental group was microinjected with a mixture of 1 μL of AAV2/Anc80L65-CMV-eGFP and Fast Green FCF dye (Sigma-Aldrich, St. Louis, MO, USA; 5:1 ratio), while each otocyst in the sham group was microinjected with 1 μL of phosphate-buffered saline (PBS) (Thermo Fisher Scientific, Waltham, MA, USA; Figure 1A). During surgery, we regularly dripped 50°C PBS onto the surface of the uterus to prevent heat loss and to allow the syringe needle to penetrate easily. After microinjection, we sequentially closed the abdominal wound in the muscular and dermal layers with surgical sutures. Mice were placed under a lamp for 5 min after surgery to recover.

Immunofluorescence Staining

First, inner ear tissue was carefully removed from mice euthanized with CO_2 (Figure 1B), perfused with 4% paraformaldehyde (PFA;

Table 1. Comparison of AAV Transduction Efficiency in the Inner Ear

Cell Types	Cochlear Hair Cells		Vestibular Hair Cells	Spiral Ganglion Neurons	References
Stage-AAV	IHCs	OHCs			
In utero-Anc80L65	91%–97%	84%–94%	92.6%	96.7%	This study
In utero-AAV1	89%–91%	84%–92%	ND	ND	Kim et al., 2016[31]
Newborn-Anc80L65	~100%	81%–95%	ND	ND	Gu et al., 2019[18]
	~100%	90%–100%	~83%	ND	Landegger et al., 2017[3]
	~94%	~67%	~67.7%	ND	Isgrig et al., 2019[7]
	ND	80%–100%	ND	ND	Pan et al., 2017[13]
Adult-Anc80L65	84%–98%	2.5%–71%	ND	ND	Tao et al., 2018[15]
	~100%	18%–90%	~38%	3%–10%	Suzuki et al., 2017[16]
	84%–91%	ND	ND	ND	Yoshimura et al., 2018[17]

ND, not described.

Bio Basic, Toronto, Canada), postfixed in the same solution for 2 h at room temperature (RT) and washed in PBS. For whole-mount studies, segments of the stria vascularis and organ of Corti together with Reissner's membrane from postnatal stage (P7) mice were dissected out of the inner ear specimens with a fine needle. The samples were permeabilized with 1% PBS/Triton X-100 (Sigma-Aldrich, St. Louis, MO, USA) for 30 min, washed with PBS, and incubated overnight at 4°C in blocking solution (5% BSA/PBS solution). The tissues were then stained with a rabbit anti-myosin VIIA primary antibody (1:100 dilution, Proteus BioScience, Redwood, CA, USA) and a goat anti-human/mouse/rat SOX2 antigen affinity-purified polyclonal antibody (1:200 dilution, R&D Systems, Minneapolis, MN, USA) together overnight. The tissues were then incubated with 4′,6-**dia**midino-2-**p**heny**l**indole (DAPI) (1:5,000; Thermo Fisher Scientific, Waltham, MA, USA), Alexa Fluor 568-conjugated goat anti-rabbit immunoglobulin G (IgG; H+L) secondary antibodies (1:200; Thermo Fisher Scientific, Waltham, MA, USA), and NorthernLights anti-goat IgG-NL637 (1:200 dilution; R&D Systems, Minneapolis, MN, USA). After washing in PBS, the tissues were mounted using a ProLong Antifade Kit (Molecular Probes, Eugene, OR, USA). Images of the tissues were acquired with a laser scanning confocal microscope (Zeiss LSM 880, Jena, Germany).

With regard to frozen sections, whole inner ears from P28 mice were decalcified for 7 days, dehydrated with gradient sucrose solutions, and then embedded in the O.C.T. compound (Sakura Finetek, Torrance, CA, USA). Next, 7-μm tissue sections of inner ears mounted on silane-coated glass slides were washed in PBS solution to remove the O.C.T. compound and submerged in proteinase K (Sigma-Aldrich, St. Louis, MO, USA) working solution (a mixture of Proteinase K and echo time [TE]-$CaCl_2$ buffer at a concentration of 20 μg/mL in TE-$CaCl_2$ buffer) for 20 min at 37°C. The sections were then permeabilized with 1% PBS/Triton X-100 for 20 min, blocked with 5% BSA/PBS solution for 30 min at RT and incubated with rabbit anti-beta III tubulin primary antibodies (1:1,000; Abcam, Burlingame, CA, USA) diluted in blocking solution at 4°C overnight. Then, the sections were incubated with DAPI (1:5,000; Thermo Fisher Scientific, Waltham, MA, USA) and Alexa Fluor 568-conjugated goat anti-rabbit IgG (H+L) secondary antibodies (1:200; Thermo Fisher Scientific, Waltham, MA, USA) at 4°C overnight. The samples were washed with PBS to remove any residual antibodies and mounted using a ProLong Antifade Kit (Molecular Probes, USA). All slides were examined by laser scanning confocal microscopy (Zeiss LSM 880, Jena, Germany).

ABR Measurement

P28–P35 mice were anesthetized with sodium pentobarbital (35 mg/kg) delivered intraperitoneally and placed in head immobilization devices within an insulated and grounded test room. We used an evoked potential detection system (Smart EP 3.90; Intelligent Hearing Systems, Miami, FL, USA) to measure the ABR thresholds in the mice. Clicks (2–4 kHz) sounds and 8, 16, and 32 kHz tone bursts at varying intensities were generated to evoke ABRs in the mice. To determine ABR thresholds, we used sound pressure levels between 25 and 60 dB. Using an alternating polarity stimulus, we collected and averaged 1,024 responses for each sound pressure level. The response signals were recorded with subcutaneous needle electrodes. The threshold was defined as the lowest dB at which peak I could be detected and

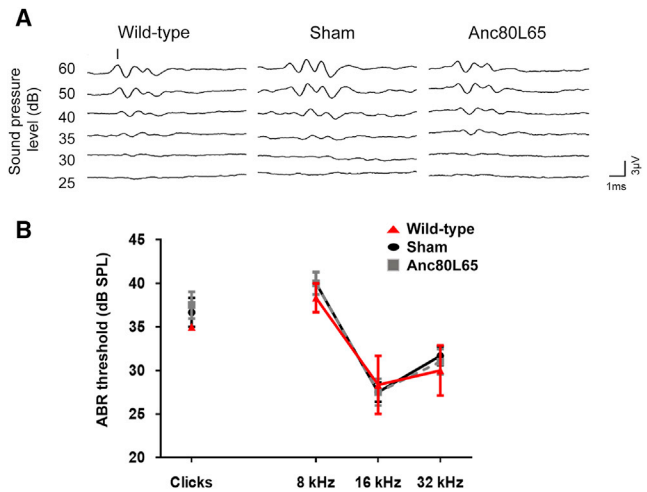

Figure 3. *In Utero* Microinjection Has Minimal Adverse Effects on Hearing
ABRs of noninjected (wild-type, n = 6), PBS-injected (sham, n = 5), and Anc80L65-injected mice (n = 5). (A) Click-evoked ABRs of wild-type (upper), sham (middle), and Anc80L65-injected (lower) mice at P28. The amplitude of the response is expressed in microvolts (μV). The time is expressed in milliseconds (ms). (B) The ABR was assessed with clicks and with tone bursts at 8 kHz, 16 kHz, and 32 kHz. No significant differences were observed among any of the tested frequencies.

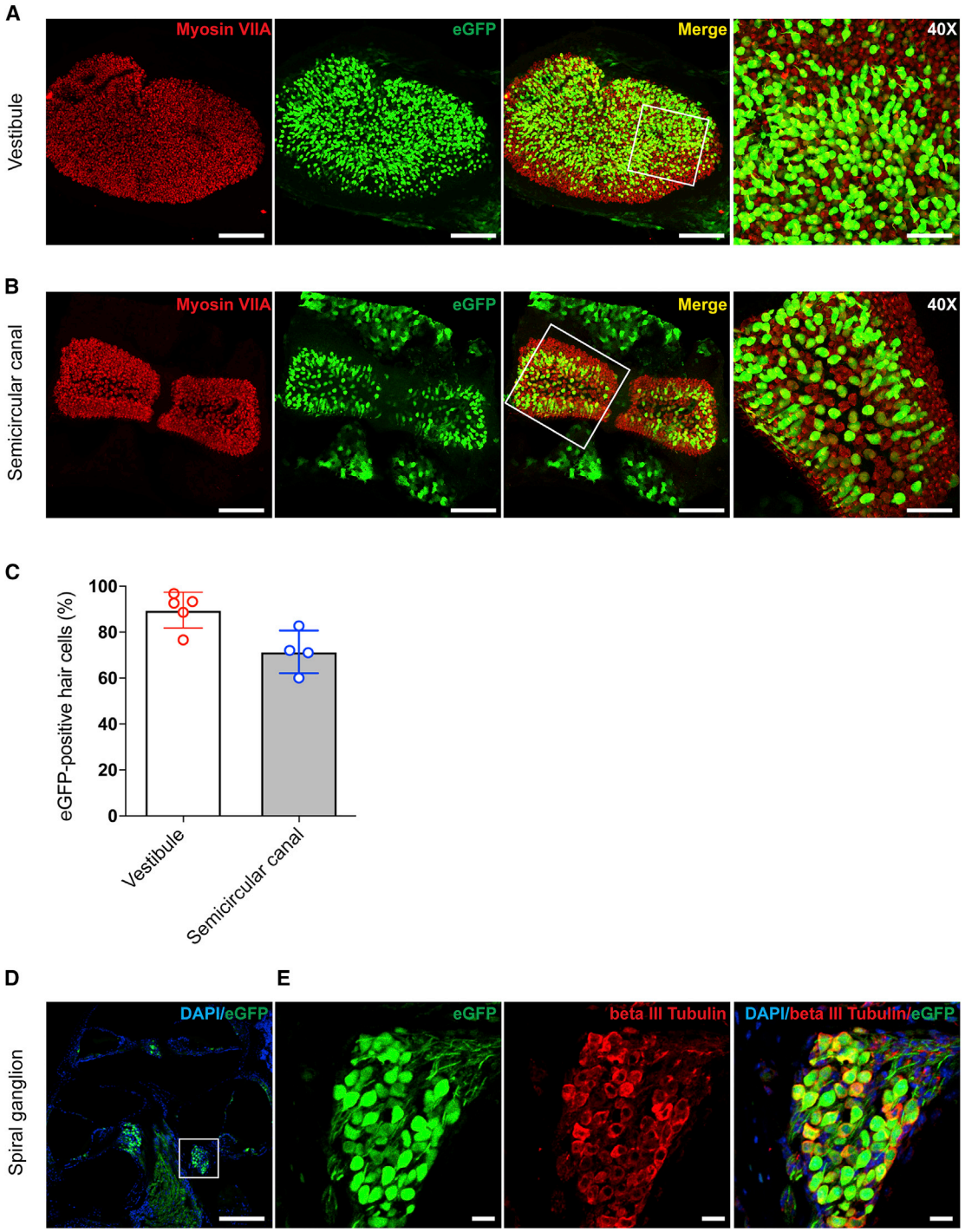

Figure 4. Anc80L65 Robustly Transduces the Vestibular and Semicircular Canals Sensory Epithelia and SGNs

(A and B) The expression of myosin VIIA (red) indicates the positions of HCs in vestibules (represented by saccules; A) and semicircular canals (represented by posterior semicircular canals; B). The proportion of eGFP-positive cells among all HCs was quantified. The scale bar represents 100 μm in the images of vestibules and semicircular canals. The scale bars in the magnified views (40×) from the areas in the white rectangles in the vestibules and semicircular canals represent 50 μm. (C) The transduction efficiency was 89.6% ± 7.8% in vestibules (n = 5) and 71.4% ± 9.3% in semicircular canals (n = 5). (D) Cross section of the cochlea at P28. (E) Magnified views of from the area in the white rectangle in (C). Beta III tubulin staining (red) indicates the distribution of SGNs, and eGFP staining indicates cells transduced by Anc80L65. The scale bar in (D) represents 200 μm, while that in (E) represents 25 μm.

reproduced with increasing sound intensities. The detailed methods were described in our previous study.[39]

Quantification of Transduced HCs and SGNs

For the quantification of cochlear HCs, we separately counted only the HCs with obvious and intact myosin VIIA and eGFP staining in 200-μm segments of sensory epithelium taken at the apical, middle, and basal turns of the cochlea. The number of myosin VIIA-stained cells in each image was divided by the number of eGFP-positive cells and is presented as a percentage ([eGFP/myosin VIIA] × 100%). For the quantification of HCs in vestibules and semicircular canals, images acquired at 40× magnification were selected for statistical analyses. The transduction efficiency in neurons was calculated as the ratio of the number of eGFP-stained cells to the number of beta III tubulin-stained cells ([eGFP/beta III tubulin] × 100%). All quantifications were performed in MetaMorph software (Molecular Devices, Sunnyvale, CA, US). We loaded the unadjusted 16-bit images into MetaMorph software, determined the intensity above the local background as a constant number, and then set the minimum and maximum widths of the cells in each image.

Statistical Analyses

The data are presented as the mean ± SD. Statistical analyses were conducted with the χ^2 test or Fisher's exact test for categorical variables and with Student's t test or ANOVA for continuous variables. A p value of < 0.05 was considered to indicate significance. All analyses were performed using SPSS/Windows software 15.0 (SPSS Science, Chicago, IL, USA).

SUPPLEMENTAL INFORMATION

Supplemental Information can be found online at https://doi.org/10.1016/j.omtm.2020.06.019.

AUTHOR CONTRIBUTIONS

Conceptualization, Y.-F.C. and J.-W.T.; Methodology, J.-W.T., H.-Y.C., and H.T.; Validation, C.-J.H., Y.-C.L., and Y.-H.T.; Formal Analysis, C.-J.H. and Y.-C.L.; Investigation, C.-J.H., Y.-C.L., Y.-H.T., C.-Y.H., and H.-Y.C.; Resources, R.X. and L.H.V.; Data Curation, C.-J.H. and Y.-C.L.; Writing – Original Draft, C.-J.H.; Writing – Review & Editing, Y.-F.C., C.-C.W., J.-W.T., and L.H.V.; Supervision, C.-J.H.; Funding Acquisition, Y.-F.C., C.-C.W., and C.-J.H.

CONFLICTS OF INTEREST

The authors declare no competing interests.

ACKNOWLEDGMENTS

We thank the staff of the Second Core Laboratory, Department of Medical Research, National Taiwan University Hospital, for technical assistance with the microscopic images. The Consortium is funded by the Ministry of Science and Technology (MOST108-2628-B075-004 and MOST106-2314-B075-081). We also thank Taipei Veterans General Hospital (V109C-135), National Taiwan University Hospital (NTUH.108-T14), and Taipei Veterans General Hospital–National Taiwan University Hospital Joint Research Program (VN107-11, VN108-09, and VN109-15) for grant support.

REFERENCES

1. Wake, M., Tobin, S., Cone-Wesson, B., Dahl, H.-H., Gillam, L., McCormick, L., Poulakis, Z., Rickards, F.W., Saunders, K., Ukoumunne, O.C., and Williams, J. (2006). Slight/mild sensorineural hearing loss in children. Pediatrics *118*, 1842–1851.

2. Feder, K.P., Michaud, D., McNamee, J., Fitzpatrick, E., Ramage-Morin, P., and Beauregard, Y. (2017). Prevalence of hearing loss among a representative sample of Canadian children and adolescents, 3 to 19 years of age. Ear Hear. *38*, 7–20.

3. Landegger, L.D., Pan, B., Askew, C., Wassmer, S.J., Gluck, S.D., Galvin, A., Taylor, R., Forge, A., Stankovic, K.M., Holt, J.R., and Vandenberghe, L.H. (2017). A synthetic AAV vector enables safe and efficient gene transfer to the mammalian inner ear. Nat. Biotechnol. *35*, 280–284.

4. Merentie, M., Lottonen-Raikaslehto, L., Parviainen, V., Huusko, J., Pikkarainen, S., Mendel, M., Laham-Karam, N., Kärjä, V., Rissanen, R., Hedman, M., and Ylä-Herttuala, S. (2016). Efficacy and safety of myocardial gene transfer of adenovirus, adeno-associated virus and lentivirus vectors in the mouse heart. Gene Ther. *23*, 296–305.

5. Osmon, K.J., Woodley, E., Thompson, P., Karumuthil-Melethil, S., Gray, S., and Walia, J. (2016). 363. Improvement of Sandhoff Phenotype Following Intravenous Injection of Adeno-Associated Viral Vector Expressing a Hexosaminidase Isoenzyme in Adult Sandhoff Mice: Preclinical Safety and Efficacy Study. Mol. Ther. *24*, S145–S146.

6. Yin, H., Kauffman, K.J., and Anderson, D.G. (2017). Delivery technologies for genome editing. Nat. Rev. Drug Discov. *16*, 387–399.

7. Isgrig, K., McDougald, D.S., Zhu, J., Wang, H.J., Bennett, J., and Chien, W.W. (2019). AAV2.7m8 is a powerful viral vector for inner ear gene therapy. Nat. Commun. *10*, 427.

8. Shibata, S.B., Ranum, P.T., Moteki, H., Pan, B., Goodwin, A.T., Goodman, S.S., Abbas, P.J., Holt, J.R., and Smith, R.J.H. (2016). RNA interference prevents autosomal-dominant hearing loss. Am. J. Hum. Genet. *98*, 1101–1113.

9. Emptoz, A., Michel, V., Lelli, A., Akil, O., Boutet de Monvel, J., Lahlou, G., Meyer, A., Dupont, T., Nouaille, S., Ey, E., et al. (2017). Local gene therapy durably restores vestibular function in a mouse model of Usher syndrome type 1G. Proc. Natl. Acad. Sci. USA *114*, 9695–9700.

10. Askew, C., Rochat, C., Pan, B., Asai, Y., Ahmed, H., Child, E., Schneider, B.L., Aebischer, P., and Holt, J.R. (2015). Tmc gene therapy restores auditory function in deaf mice. Sci. Transl. Med *7*, 295ra108.

11. Akil, O., Seal, R.P., Burke, K., Wang, C., Alemi, A., During, M., Edwards, R.H., and Lustig, L.R. (2012). Restoration of hearing in the VGLUT3 knockout mouse using virally mediated gene therapy. Neuron *75*, 283–293.

12. Chang, Q., Wang, J., Li, Q., Kim, Y., Zhou, B., Wang, Y., Li, H., and Lin, X. (2015). Virally mediated Kcnq1 gene replacement therapy in the immature scala media restores hearing in a mouse model of human Jervell and Lange-Nielsen deafness syndrome. EMBO Mol. Med. *7*, 1077–1086.

13. Pan, B., Askew, C., Galvin, A., Heman-Ackah, S., Asai, Y., Indzhykulian, A.A., Jodelka, F.M., Hastings, M.L., Lentz, J.J., Vandenberghe, L.H., et al. (2017). Gene therapy restores auditory and vestibular function in a mouse model of Usher syndrome type 1c. Nat. Biotechnol. *35*, 264–272.

14. Chien, W.W., McDougald, D.S., Roy, S., Fitzgerald, T.S., and Cunningham, L.L. (2015). Cochlear gene transfer mediated by adeno-associated virus: Comparison of two surgical approaches. Laryngoscope *125*, 2557–2564.

15. Tao, Y., Huang, M., Shu, Y., Ruprecht, A., Wang, H., Tang, Y., Vandenberghe, L.H., Wang, Q., Gao, G., Kong, W.J., and Chen, Z.Y. (2018). Delivery of adeno-associated virus vectors in adult mammalian inner-ear cell subtypes without auditory dysfunction. Hum. Gene Ther. *29*, 492–506.

16. Suzuki, J., Hashimoto, K., Xiao, R., Vandenberghe, L.H., and Liberman, M.C. (2017). Cochlear gene therapy with ancestral AAV in adult mice: complete transduction of inner hair cells without cochlear dysfunction. Sci. Rep. *7*, 45524.

17. Yoshimura, H., Shibata, S.B., Ranum, P.T., and Smith, R.J.H. (2018). Enhanced viral-mediated cochlear gene delivery in adult mice by combining canal fenestration with round window membrane inoculation. Sci. Rep. *8*, 2980.

18. Gu, X., Chai, R., Guo, L., Dong, B., Li, W., Shu, Y., Huang, X., and Li, H. (2019). Transduction of Adeno-Associated Virus Vectors Targeting Hair Cells and Supporting Cells in the Neonatal Mouse Cochlea. Front. Cell. Neurosci. *13*, 8.

19. Tan, F., Chu, C., Qi, J., Li, W., You, D., Li, K., Chen, X., Zhao, W., Cheng, C., Liu, X., et al. (2019). AAV-ie enables safe and efficient gene transfer to inner ear cells. Nat. Commun. *10*, 3733.

20. Bedrosian, J.C., Gratton, M.A., Brigande, J.V., Tang, W., Landau, J., and Bennett, J. (2006). In vivo delivery of recombinant viruses to the fetal murine cochlea: transduction characteristics and long-term effects on auditory function. Mol. Ther. *14*, 328–335.

21. Zinn, E., Pacouret, S., Khaychuk, V., Turunen, H.T., Carvalho, L.S., Andres-Mateos, E., Shah, S., Shelke, R., Maurer, A.C., Plovie, E., et al. (2015). In silico reconstruction of the viral evolutionary lineage yields a potent gene therapy vector. Cell Rep. *12*, 1056–1068.

22. Nist-Lund, C.A., Pan, B., Patterson, A., Asai, Y., Chen, T., Zhou, W., Zhu, H., Romero, S., Resnik, J., Polley, D.B., et al. (2019). Improved TMC1 gene therapy restores hearing and balance in mice with genetic inner ear disorders. Nat. Commun. *10*, 236.

23. Stickrod, G. (1981). In utero injection of rat fetuses. Physiol. Behav. *27*, 557–558.

24. Coutelle, C. (2018). An important step on the long path to clinical application of in utero gene therapy. Gene Ther. *25*, 451–453.

25. Lu, Y.C., Wu, C.C., Shen, W.S., Yang, T.H., Yeh, T.H., Chen, P.J., Yu, I.S., Lin, S.W., Wong, J.M., Chang, Q., et al. (2011). Establishment of a knock-in mouse model with the SLC26A4 c.919-2A>G mutation and characterization of its pathology. PLoS ONE *6*, e22150.

26. Wang, Q.J., Zhao, Y.L., Rao, S.Q., Guo, Y.F., He, Y., Lan, L., Yang, W.Y., Zheng, Q.Y., Ruben, R.J., Han, D.Y., and Shen, Y. (2011). Newborn hearing concurrent gene screening can improve care for hearing loss: a study on 14,913 Chinese newborns. Int. J. Pediatr. Otorhinolaryngol. *75*, 535–542.

27. MacKenzie, T.C., Kobinger, G.P., Kootstra, N.A., Radu, A., Sena-Esteves, M., Bouchard, S., Wilson, J.M., Verma, I.M., and Flake, A.W. (2002). Efficient transduction of liver and muscle after in utero injection of lentiviral vectors with different pseudotypes. Mol. Ther. *6*, 349–358.

28. DeWeerdt, S. (2018). Prenatal gene therapy offers the earliest possible cure. Nature *564*, S6–S8.

29. Gubbels, S.P., Woessner, D.W., Mitchell, J.C., Ricci, A.J., and Brigande, J.V. (2008). Functional auditory hair cells produced in the mammalian cochlea by in utero gene transfer. Nature *455*, 537–541.

30. Miwa, T., Minoda, R., Ise, M., Yamada, T., and Yumoto, E. (2013). Mouse otocyst transuterine gene transfer restores hearing in mice with connexin 30 deletion-associated hearing loss. Mol. Ther. *21*, 1142–1150.

31. Kim, M.-A., Cho, H.-J., Bae, S.-H., Lee, B., Oh, S.-K., Kwon, T.-J., Ryoo, Z.Y., Kim, H.Y., Cho, J.H., Kim, U.K., and Lee, K.Y. (2016). Methionine sulfoxide reductase B3-targeted in utero gene therapy rescues hearing function in a mouse model of congenital sensorineural hearing loss. Antioxid. Redox Signal. *24*, 590–602.

32. Liu, Y., Okada, T., Sheykholeslami, K., Shimazaki, K., Nomoto, T., Muramatsu, S., Kanazawa, T., Takeuchi, K., Ajalli, R., Mizukami, H., et al. (2005). Specific and efficient transduction of Cochlear inner hair cells with recombinant adeno-associated virus type 3 vector. Mol. Ther. *12*, 725–733.

33. Stojanova, Z.P., Kwan, T., and Segil, N. (2015). Epigenetic regulation of Atoh1 guides hair cell development in the mammalian cochlea. Development *142*, 3529–3536.

34. Yu, K.S., Frumm, S.M., Park, J.S., Lee, K., Wong, D.M., Byrnes, L., Knox, S.M., Sneddon, J.B., and Tward, A.D. (2019). Development of the Mouse and Human Cochlea at Single Cell Resolution. bioRxiv. https://doi.org/10.1101/739680.

35. Kaga, K. (2014). Gene Mutation in Congenital Deafness and Vestibular Failure (Vertigo and Balance Disorders in Children), pp. 79–84.

36. Smith, R.J., Bale, J.F., Jr., and White, K.R. (2005). Sensorineural hearing loss in children. Lancet *365*, 879–890.

37. Hoefsloot, L.H., Feenstra, I., Kunst, H.P., and Kremer, H. (2014). Genotype phenotype correlations for hearing impairment: approaches to management. Clin. Genet. *85*, 514–523.

38. Wang, L., Jiang, H., and Brigande, J.V. (2012). Gene transfer to the developing mouse inner ear by in vivo electroporation. J. Vis. Exp *30*, 3653.

39. Lu, Y.-C., Wu, C.-C., Yang, T.-H., Lin, Y.-H., Yu, I.-S., Lin, S.-W., Chang, Q., Lin, X., Wong, J.M., and Hsu, C.J. (2013). Differences in the pathogenicity of the p.H723R mutation of the common deafness-associated SLC26A4 gene in humans and mice. PLoS ONE *8*, e64906.

40. Ryotaro, Omichi, Hidekane, Yoshimura, Seiji, B., Shibata, Luk, H., Vandenberghe, and Richard, J H Smith (2020). Hair Cell Transduction Efficiency of Single- and Dual-AAV Serotypes in Adult Murine Cochleae. Molecular Therapy — Methods & Clinical Development *13*, 1167–1177.

41. Bence, György, Elise, J., Meijer, Maryna, V., Ivanchenko, Kelly, Tenneson, Frederick, Emond, Killian, S., Hanlon., et al. (2018). Gene Transfer with AAV9-PHP.B Rescues Hearing in a Mouse Model of Usher Syndrome 3A and Transduces Hair Cells in a Non-human Primate. Molecular Therapy — Methods & Clinical Development *20*, 1–13.

42. Kim, Min-A, Ryu, Nari, Kim, Hye-Min, Kim, Ye-Ri, Lee, Byeonghyeon, Kwon, Tae-Jun., et al. (2019). Targeted Gene Delivery into the Mammalian Inner Ear Using Synthetic Serotypes of Adeno-Associated Virus Vectors. Molecular Therapy — Methods & Clinical Development *11*, 197–204.

OMTM, Volume *18*

Supplemental Information

Efficient in Utero Gene Transfer to the Mammalian Inner Ears by the Synthetic Adeno-Associated Viral Vector Anc80L65

Chin-Ju Hu, Ying-Chang Lu, Yi-Hsiu Tsai, Haw-Yuan Cheng, Hiroki Takeda, Chun-Ying Huang, Ru Xiao, Chuan-Jen Hsu, Jin-Wu Tsai, Luk H. Vandenberghe, Chen-Chi Wu, and Yen-Fu Cheng

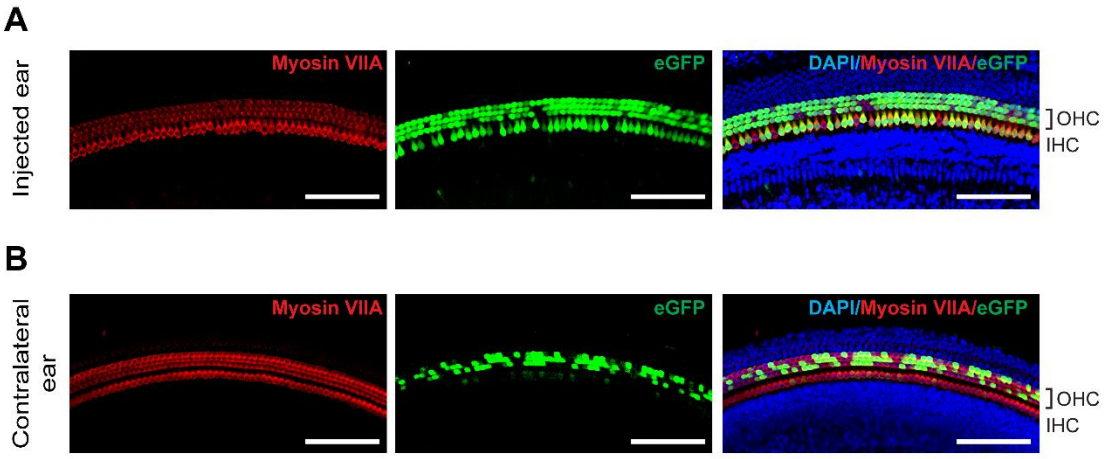

Supplementary Figure 1. Transduction of contralateral cochlea with Anc80L65. eGFP expression was observed in the injected and contralateral ears at P7. The transduction in the contralateral cochleas was weak and sporadic compared to that in the injected ears. In the injected ears, a high transduction rate was observed (A). In the contralateral ears, an eGFP signal was observed but was much weaker than that in the injected ear (B). The transduction rates in the contralateral ears were 26.6±29.5% for IHC and 40.4±38.5% for OHC (n=5). Red indicates myosin VIIA, green indicates eGFP, and blue indicates DAPI. The bar represents 100 μm in each image.